

See discussions, stats, and author profiles for this publication at: <https://www.researchgate.net/publication/232933878>

Structures and magnetism of multinuclear vanadium–pentacene sandwich clusters and their 1D molecular wires

ARTICLE *in* THE JOURNAL OF CHEMICAL PHYSICS · OCTOBER 2012

Impact Factor: 2.95 · DOI: 10.1063/1.4759505 · Source: PubMed

CITATIONS

5

READS

36

5 AUTHORS, INCLUDING:



Tingting Zhang

Fudan University

47 PUBLICATIONS 481 CITATIONS

SEE PROFILE



Liyan Zhu

National University of Singapore

32 PUBLICATIONS 372 CITATIONS

SEE PROFILE



Qisheng Wu

Southeast University (China)

5 PUBLICATIONS 16 CITATIONS

SEE PROFILE



Shuo-Wang Yang

Agency for Science, Technology and Research...

41 PUBLICATIONS 656 CITATIONS

SEE PROFILE

Structures and magnetism of multinuclear vanadium-pentacene sandwich clusters and their 1D molecular wires

Tingting Zhang, Liyan Zhu, Qisheng Wu, Shuo-Wang Yang, and Jinlan Wang

Citation: *The Journal of Chemical Physics* **137**, 164309 (2012); doi: 10.1063/1.4759505

View online: <http://dx.doi.org/10.1063/1.4759505>

View Table of Contents: <http://scitation.aip.org/content/aip/journal/jcp/137/16?ver=pdfcov>

Published by the [AIP Publishing](#)

Articles you may be interested in

[LiFe₂Cl_n \(n=4–6\) clusters: Double-exchange mediated molecular magnets](#)

Appl. Phys. Lett. **105**, 163112 (2014); 10.1063/1.4900421

[Weak antiferromagnetic coupling in molecular ring is predicted correctly by density functional theory plus Hubbard U](#)

J. Chem. Phys. **132**, 244104 (2010); 10.1063/1.3421645

[Cyanide-bridged Ru_xNi_{3-3x/2}\[Cr\(CN\)₆\]₂·zH₂O molecular magnets: Controlling structural disorder and magnetic properties by a 4d ion \(ruthenium\) substitution](#)





J. Appl. Phys. **107**, 053902 (2010); 10.1063/1.3311966

[Magnetism in Molecular VanadiumBenzene Sandwiches](#)

AIP Conf. Proc. **786**, 444 (2005); 10.1063/1.2103906

[Effect of oxygen vacancies on the magnetic structure of the La_{0.6}Sr_{0.4}FeO_{3-δ} perovskite: A neutron diffraction study](#)

J. Appl. Phys. **91**, 7938 (2002); 10.1063/1.1455613

 **The Journal of
Chemical Physics**
Meet The New Deputy Editors
 **Peter Hamm**  **David E. Manolopoulos**  **James L. Skinner**

Structures and magnetism of multinuclear vanadium-pentacene sandwich clusters and their 1D molecular wires

Tingting Zhang,¹ Liyan Zhu,¹ Qisheng Wu,¹ Shuo-Wang Yang,² and Jinlan Wang^{1,a)}

¹Department of Physics, Southeast University, Nanjing 211189, People's Republic of China

²Institute of High Performance Computing, Agency for Science, Technology and Research, 1 Fusionopolis Way, #16-16 Connexis, Singapore 138632, Singapore

(Received 21 July 2012; accepted 2 October 2012; published online 25 October 2012)

Two types of multinuclear sandwich clusters, $(V_3)_n\text{Pen}_{n+1}$, $(V_4)_n\text{Pen}_{n+1}$ (Pen = Pentacene; $n = 1, 2$), and their corresponding infinite one-dimensional (1D) molecular wires $[(V_3\text{Pen})_\infty]$, $[(V_4\text{Pen})_\infty]$ are investigated theoretically, especially on their magnetic coupling mechanism. These sandwich clusters and molecular wires are found to be of high stability and exhibit intriguing magnetic properties. The intra-layered V atoms in $(V_3)_n\text{Pen}_{n+1}$ clusters prefer antiferromagnetic (AFM) coupling, while they can be either ferromagnetic (FM) or AFM coupling in $(V_4)_n\text{Pen}_{n+1}$ depending on the intra-layered V-V distances via direct exchange or superexchange mechanism. The inter-layered V atoms favor FM coupling in $(V_3)_2\text{Pen}_3$, whereas they are AFM coupled in $(V_4)_2\text{Pen}_3$. Such magnetic behaviors are the consequence of the competition between direct exchange and superexchange interactions among inter-layered V atoms. In contrast, the 1D molecular wires, $[(V_3\text{Pen})_\infty]$ and $[(V_4\text{Pen})_\infty]$, appear to be FM metallic with ultra high magnetic moments of 6.8 and 4.0 μ_B per unit cell respectively, suggesting that they can be served as good candidates for molecular magnets. © 2012 American Institute of Physics. [<http://dx.doi.org/10.1063/1.4759505>]

I. INTRODUCTION

Since the discovery of ferrocene,^{1,2} huge efforts have been invested on transition metal (TM)–cyclic organic molecule sandwich clusters due to their unique structural and intriguing electronic, magnetic, and optical properties. Many experimental^{3–8} and theoretical^{9–22} works have reported that a wide variety of organic ligands are able to form stable multidecker sandwich clusters with suitable metals, such as TM-Bz (Bz = benzene, TM = Sc-Ni),¹⁹ and Ln-COT (COT = cyclooctatetraene, Ln = Eu, Tb, Ho, Tm).⁸ These clusters exhibit unusual magnetic properties. For example, the magnetic moment of $V_n\text{Bz}_{n+1}$ increases linearly along with the size;¹³ $\text{Eu}_n\text{COT}_{n+1}$ possess extraordinarily high magnetic moments and high spin filter efficiency;^{14,23} hybrid $\text{TM}_n(\text{FeCp}_2)_{n+1}$ clusters show significant magnetic moment enhancement as compared to their constituted monometallic counterparts.^{15,21,24} In addition, many infinite 1D sandwich molecular wires exhibit exceptional high spin filter efficiency, which are important in the application of spintronics.^{11,23,25}

However, previous studies mostly focused on mononuclear metal center sandwich clusters. Planar aromatic ligands can accommodate two or more TMs to form stable multinuclear metal center sandwich structures, and a few efforts have been dedicated to this field both experimentally^{26–30} and theoretically.^{31–35} Theoretical calculations³⁶ predicted that three Ni atoms can be sandwiched by two Bz molecules to form a stable D_{3h} structure. Larger planar aromatic hydrocarbon ligands, such as cycloheptatrienyl (C_7H_7),²⁶ cyclooctatetraene (C_8H_8),²⁷ pentalene (C_8H_6),³⁷ naphthalene (C_{10}H_8),³⁸ anthracene ($\text{C}_{14}\text{H}_{10}$),²⁴ pyrene ($\text{C}_{16}\text{H}_{10}$),³⁹ and

tetracene ($\text{C}_{18}\text{H}_{12}$),³⁹ can encompass more TMs between two ligands to form stable sandwich clusters. As an extreme example, nine Pd atoms can be sandwiched by two tetracenes ($\text{C}_{18}\text{H}_{12}$).³⁹ These multinuclear sandwich clusters and their 1D molecular wires often exhibit different magnetic properties from those mononuclear ones. For instance, experimental studies revealed that the bi-metal center sandwich clusters TM_2Pn_2 (Pn = pentalene, TM = Co and Ni) are diamagnetic, while their mononuclear metal center counterparts, TMCP_2 (Cp = cyclopentadienyl), are paramagnetic.^{40,41} Theoretical studies have also showed that $[(V_2\text{Pn})_\infty]$ and $[(\text{Cr}_2\text{Pn})_\infty]$ molecular wires are AFM (antiferromagnetic) semiconductors,⁴² which are totally different from the half-metallic features of their corresponding mononuclear analogues $[(V\text{Cp})_\infty]$ and $[(\text{CrCp})_\infty]$ molecular wires.¹⁶

These sandwich clusters are suggested as ideal candidates for the possible smallest molecular magnets.⁴³ However, the magnetic coupling mechanism between TMs among these sandwich molecular clusters or wires still remains unclear, which actually is crucial to further exploration in new sandwich molecular clusters/wires and their applications. Pentacene (Pen), a linearly fused planar aromatic structure with five benzene rings, was first synthesized in 1912 with catalytic amounts of AlCl_3 .⁴⁴ Compared with benzene or naphthalene (Np), Pen can accommodate more metal atoms, which would provide a way to study how the metal-metal interactions affect the magnetism of sandwich clusters. Moreover, another advantage of Pen over benzene is that Pen can strongly bond to some substrate like Si (100).⁴⁵ Thus, we can effectively deposit the V-Pen sandwich clusters onto the substrate with controllable orientation for practical application. In the present work, two kinds of sandwich clusters, with three or four V atoms sandwiched between Pen ligands, $(V_3)_n\text{Pen}_{n+1}$ and

^{a)}Electronic mail: jlwang@seu.edu.cn.

$(V_4)_n\text{Pen}_{n+1}$ ($n = 1, 2$), are studied to explore the metal coupling mechanism. In addition, their 1D molecular wires $[\text{V}_3\text{Pen}]_\infty$ and $[\text{V}_4\text{Pen}]_\infty$ are also investigated. It is found that intra-layered V atoms in $(V_3)_n\text{Pen}_{n+1}$ are AFM coupled, while they are either FM (ferromagnetic) or AFM (antiferromagnetic) coupled in $(V_4)_n\text{Pen}_{n+1}$ depending on the V-V distance. However, inter-layered V atoms are FM coupled in $(V_3)_n\text{Pen}_{n+1}$ and AFM coupled in $(V_4)_n\text{Pen}_{n+1}$. Differently, in 1D $[\text{V}_3\text{Pen}]_\infty$ and $[\text{V}_4\text{Pen}]_\infty$ molecular wires, all V atoms are FM coupled with ultra high magnetic moments.

II. COMPUTATIONAL METHOD

Calculations on the finite sandwich clusters were performed using gradient corrected density functional theory (DFT) of Becke-Lee-Yang-Parr^{46,47} functional combined with double numerical basis set with polarization functions as implemented in the DMol³ package.^{48,49} Density functional semi-core pseudo-potentials were adopted to describe the interactions between valence electrons and ionic core. All sandwich clusters were optimized using the Broyden-Fletcher-Goldfarb-Shanno algorithm without any symmetry constraint. The convergences for gradient, displacement, and total energy were 10^{-3} , 10^{-3} , and 10^{-5} a.u., respectively. To locate the ground spin state for each geometry, the magnetic moment was first allowed to freely optimize to the favored spin states; the neighboring spin states were further optimized by fixing the magnetic moment. These two steps ensure that the obtained spin states are the energetically most favorable ones. We have also calculated the vibrational frequencies of the most stable structures for the small clusters, e.g., V_3Pen_2 and V_4Pen_2 clusters, and they are positive, indicating that they are true local minima. The local magnetic moments on each atom were obtained by Hirshfeld population method.⁵⁰ To verify the reliability of the chosen functional and basis sets, we optimized VBz and $\text{V}_n\text{Bz}_{n+1}$ ($n = 1, 2$) clusters, and compared their geometric parameters, binding energies (BEs) and ionization energies, with previous theoretical and experimental reports. As shown in the supplementary material,⁵¹ our calculated results are in good agreement with earlier reported values.^{12,13,17,19,52-57} Therefore, the functional and basis sets used in current work should be appropriate for the studied sandwich clusters.

DFT results for 1D molecular wires $[\text{V}_3\text{Pen}]_\infty$ and $[\text{V}_4\text{Pen}]_\infty$ were calculated by using the Vienna Ab Initio Simulation Package (VASP).^{58,59} The spin polarized general gradient approximation with Perdew-Burke-Ernzerhof⁶⁰ functional was employed. Projected augmented wave^{61,62} pseudopotential was used to describe the electron-core interaction. The cutoff energy for plane waves was set to be 450 eV. The structures were fully relaxed with no restriction by a conjugate gradient algorithm until the Hellmann-Feynman force on each atom was less than 0.02 eV/Å. To identify the magnetic ordering of the ground state, both $1 \times 1 \times 2$ supercells of $[\text{V}_3\text{Pen}]_\infty$ and $[\text{V}_4\text{Pen}]_\infty$ molecular wires were placed in an orthogonal cell with a dimension of $25 \times 15 \times c$ Å³, where c is the lattice constant along the periodic direction of 1D molecular wire, while the lattice constants a (25 Å) and b (15 Å) are large enough to prevent

interaction between adjacent units. All possible alignments of magnetic moments were considered. The 1D Brillouin-zone grid was sampled by a $1 \times 1 \times 15$ k-point grid using the Monkhorst-Pack⁶³ scheme. Band structures and density of states (DOS) of two kinds of molecular wires were calculated using the basic unit cell since both $[\text{V}_3\text{Pen}]_\infty$ and $[\text{V}_4\text{Pen}]_\infty$ molecular wires favor FM coupling.

III. RESULTS AND DISCUSSION

A. Sandwich clusters

For $(V_3)_n\text{Pen}_{n+1}$, three intra-layered V atoms are located at the hollow sites of the first, third, and fifth hexagonal rings; while the four intra-layered V atoms in $(V_4)_n\text{Pen}_{n+1}$ are positioned at the hollow sites of the first, second, fourth, and fifth hexagonal rings. Their optimized ground state structures and their corresponding bond lengths are depicted in Fig. 1 (for the convenience of the following discussion, we numbered the V atoms) and the supplementary material;⁵¹ and their structural, electronic, and magnetic properties as well as additional two low-lying isomers are summarized in Table I. Our calculations show that the optimized sandwich clusters are slightly deformed with the rings on both ends of Pen bending slightly toward the V atoms.

To evaluate the relative stability of these multinuclear sandwich clusters, we calculate the binding energies (BEs) of $(V_3)_n\text{Pen}_{n+1}$ and $(V_4)_n\text{Pen}_{n+1}$ with respect to the isolated V atom and Pen molecule, based on the following formula:

$$\text{BE}((V_m)_n\text{Pen}_{n+1}) = m^*n^*E(V) + (n+1)^*E(\text{Pen}) - E((V_m)_n\text{Pen}_{n+1}), \quad m = 3, 4; n = 1, 2, \quad (1)$$

where $E(\cdot)$ represents the total energy of isolated V atom, fully relaxed Pen molecule, and $(V_m)_n\text{Pen}_{n+1}$ sandwich clusters at ground states, respectively. The BEs of the V_3Pen_2 , $(\text{V}_3)_2\text{Pen}_3$, V_4Pen_2 , and $(\text{V}_4)_2\text{Pen}_3$ clusters are as high as

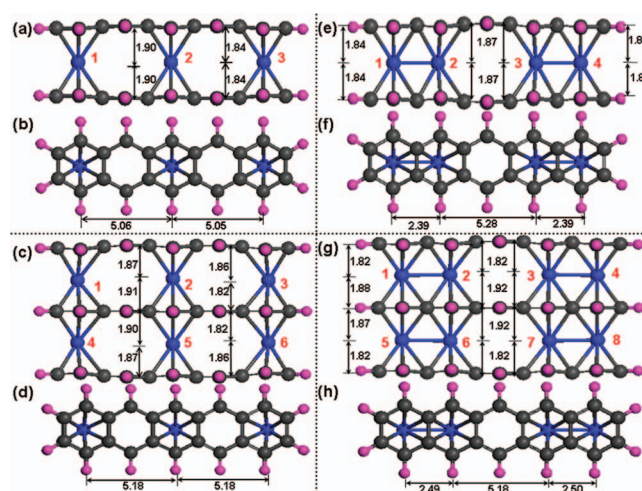


FIG. 1. Side and top views of the optimized ground state structures of V_3Pen_2 [(a) and (b)], $(\text{V}_3)_2\text{Pen}_3$ [(c) and (d)], V_4Pen_2 [(e) and (f)], and $(\text{V}_4)_2\text{Pen}_3$ [(g) and (h)] sandwich clusters, respectively. The distances between V atoms and the corresponding hexagonal ring centers (in Å) as well as the V atoms are labeled. Gray ball: C; blue ball: V; magenta: H.

TABLE I. Electronic and magnetic properties of the optimized ground state and two low-lying states of $(V_3)_n\text{Pen}_{n+1}$ and $(V_4)_n\text{Pen}_{n+1}$ ($n = 1, 2$) sandwich clusters. Point group symmetry (PGS), total magnetic moment M_t (μ_B), relative energy differences with respect to the ground state structures ΔE (eV), binding energy BE (eV), HOMO-LUMO gap Δ_{gap} (eV), and the local magnetic moment on each V atom M_{V1} - M_{V8} (μ_B).

System	PGS	M_t	ΔE	BE	Δ_{gap}	M_{V1}	M_{V2}	M_{V3}	M_{V4}	M_{V5}	M_{V6}	M_{V7}	M_{V8}
$V_3\text{Pen}_2$	D_{2h}	1	0.00	12.87	0.38	1.68	-2.17	1.66					
	D_{2h}	3	0.14	12.72	0.12	1.79	-1.52	1.79					
	D_{2h}	5	0.26	12.60	0.45	1.53	1.26	1.52					
$(V_3)_2\text{Pen}_3$	C_{2v}	2	0.00	22.80	0.51	1.62	-2.16	1.62	1.65	-2.16	1.65		
	C_s	4	0.27	22.56	0.23	-0.95	2.01	1.55	1.79	-2.21	1.66		
	C_2	6	0.02	22.80	0.39	1.46	1.89	1.46	1.71	-2.28	1.71		
$V_4\text{Pen}_2$	D_{2h}	0	0.00	17.20	0.70	0.44	0.58	-0.58	-0.44				
	D_{2h}	2	0.002	17.20	0.66	0.43	0.58	0.58	0.44				
	D_{2h}	4	0.48	16.73	0.07	0.97	1.35	0.57	0.46				
$(V_4)_2\text{Pen}_3$	C_{2h}	0	0.00	30.60	0.19	0.48	0.56	-0.59	-0.45	-0.44	-0.60	0.56	0.48
	C_s	2	0.01	30.59	0.20	0.48	0.52	0.59	0.43	-0.38	-0.70	0.55	0.49
	C_s	4	0.04	30.55	0.14	0.49	0.51	0.56	0.43	0.43	0.55	0.52	0.49

12.87, 22.80, 17.20, and 30.60 eV, respectively, indicating that they are of high stability (Table I). Moreover, the average BEs per V atom of these four sandwich clusters are 4.29, 3.80, 4.30, and 3.83 eV, respectively, which are comparable to those of VBz_2 (4.63 eV) and V_2Bz_3 (4.03 eV). This indicates that the V-Pen clusters have high stability as $\text{V}_n\text{Bz}_{n+1}$ and could be experimentally feasible.

Next, we explore the magnetic properties of V-Pen clusters. Some energetically low-lying isomers with different spin states are identified within a small energy range (<0.1 eV, shown in the supplementary material⁵¹), which suggests their potential application in magnetic storage under an external applied electric field. For $(V_3)_n\text{Pen}_{n+1}$, the magnetic moments of the V atoms are around $2.0 \mu_B$ and the middle V atoms possess larger spins than the terminal ones, whereas the Pen ligands only have small spins ($<0.25 \mu_B$). The small nonzero spins on the Pen ligands and nonintegral magnetic moments on the V atoms are mainly due to a slight charge transfer from V atoms to Pen ligands. Moreover, in the ground state, the two neighboring intra-layered V atoms in $(V_3)_n\text{Pen}_{n+1}$ favor AFM coupling, while the inter-layered V atoms are FM coupled, and the total magnetic moments of $V_3\text{Pen}_2$ and $(V_3)_2\text{Pen}_3$ are 1.0 and $2.0 \mu_B$, respectively.

Such magnetic ordering in $(V_3)_n\text{Pen}_{n+1}$ clusters can be understood from their “constituted” subunits (the optimized structural parameters of relevant sandwich clusters are presented in the supplementary material⁵¹). As shown in Fig. 2(a), the mononuclear VBz_2 cluster with a local magnetic moment of nearly $1.0 \mu_B$ on V atom can be viewed as the building block. When two VBz_2 clusters fuse together to form a V_2Ant_2 cluster via CH fragments, the two V atoms in the V_2Ant_2 favor AFM coupling, which agrees with an earlier report.²⁴ Furthermore, a pair of neighboring V atoms in the $V_3\text{Pen}_2$ cluster, which can be treated as the two V atoms in the V_2Ant_2 cluster, also prefer AFM coupling. The AFM magnetic coupling is the result of superexchange^{64,65} interaction which is illustrated in detail below. On the other hand, the inter-layered V atoms in both $\text{V}_n\text{Bz}_{n+1}$ and $(V_2)_n\text{Ant}_{n+1}$ tend to be FM coupled through the competition between direct exchange and superexchange interactions, similar to that in the V-Bz infinite wire.⁶⁶ Similarly, the inter-layered V atoms

in $(V_3)_n\text{Pen}_{n+1}$ clusters also prefer FM coupling which is a result of the competition between direct exchange and superexchange interactions mediated by the Pen ligands which is clearly displayed in Fig. 2(a).

Considering the complexity of $(V_3)_n\text{Pen}_{n+1}$ clusters and their similar magnetic coupling mechanism with $(V_2)_n\text{Ant}_{n+1}$ clusters, we further explore the frontier orbitals of the relatively simple V_2Ant_2 to address the AFM coupling mechanism between the intra-layered V atoms. As shown in Fig. 2(b), all of the ten occupied frontier orbitals of the V_2Ant_2 are doubly degenerate. The degenerate highest occupied molecular orbital (HOMO) and HOMO-1 orbitals are mainly contributed by the d_{yz} orbitals of both V atoms, and

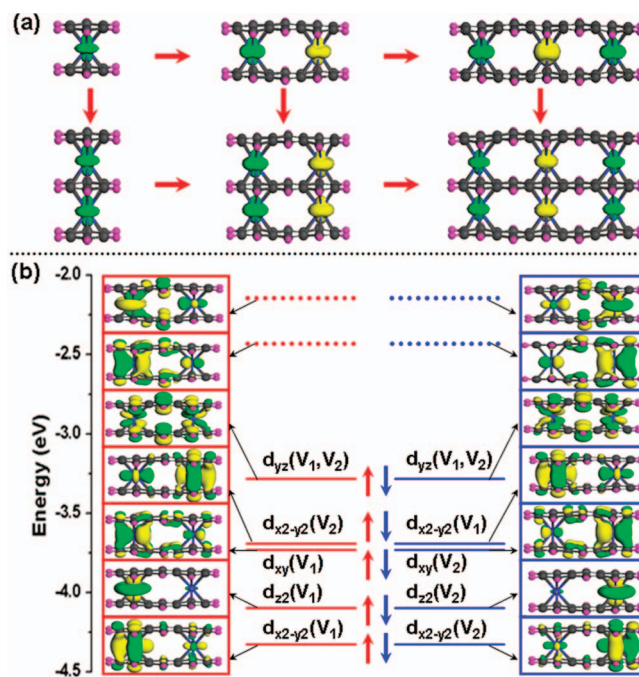


FIG. 2. (a) Spin densities of VBz_2 , V_2Ant_2 , $V_3\text{Pen}_2$, V_2Bz_3 , $(\text{V}_2)_2\text{Ant}_3$, and $(\text{V}_3)_2\text{Pen}_3$. (b) The energy levels and their corresponding occupied frontier orbitals of V_2Ant_2 . The red and blue lines refer to two different spin orbitals; the solid and dotted lines stand for occupied and unoccupied orbitals; the up and down arrows represent spin up and spin down electrons, respectively.

they are fully occupied and have no contribution to the magnetism of the whole cluster. While the remaining eight occupied frontier orbitals are mainly comprised of three α -spin d_{xy} , d_{z^2} , and $d_{x^2-y^2}$ orbitals and one β -spin $d_{x^2-y^2}$ orbital of V_1 atom, and three β -spin electrons d_{xy} , d_{z^2} , and $d_{x^2-y^2}$ orbitals and one α -spin $d_{x^2-y^2}$ orbital of V_2 atom. Since the number of valence electrons of each V atom is 5, hence, the net local magnetic moments on V_1 and V_2 atoms are around 2.0 and $-2.0 \mu_B$, respectively (1.64 and $-1.64 \mu_B$ for V_1 and V_2 atom in $V_2\text{Ant}_2$, respectively, are in agreement with 1.76 , $-1.76 \mu_B$ reported earlier²⁴). Additionally, as seen from Fig. 2(b), the magnetic moment on V atom is mostly contributed by the d_{xy} and d_{z^2} orbitals. The interaction between d_{xy} orbitals of V_1 and V_2 atoms is clearly mediated by the p orbitals of both ligands. Therefore, the V_1 - V_2 interaction is through bond exchange coupling. So the neighboring intra-layered V atoms of $(V_3)_n\text{Pen}_{n+1}$ are AFM coupled whereas the inter-layered V atoms are FM coupled.

The situation in $(V_4)_n\text{Pen}_{n+1}$ clusters becomes more complicated. The local magnetic moments of the V atoms are much smaller in $(V_4)_n\text{Pen}_{n+1}$ (around $0.5 \mu_B$), where Pen ligands also show some small magnetic moment due to some charges transferred from V atoms. Here, the V_1 (V_3) and V_2 (V_4) in $V_4\text{Pen}_2$ cluster are directly FM coupled; and the pairs of V dimers (V_1 - V_2 and V_3 - V_4) are AFM coupled as shown in Fig. 3 and Table I. For the multidecker $(V_4)_2\text{Pen}_3$ cluster, the intra-layered V atoms behave similarly to those of $V_4\text{Pen}_2$, whereas the V_1 - V_2 pair is AFM coupled with the V_3 - V_4

pair, and the inter-layered V-V pairs are also AFM coupled (Fig. 3(b)). Moreover, the small local spins of V might stem from the strong intra-layered V-V bonding in $(V_4)_n\text{Pen}_{n+1}$ which weakens the intra-atom exchange splitting of the $3d$ orbitals in V atoms. Similar results were observed in $[V_2\text{Np}]_\infty$ molecular wire when extra electrons were added.⁶⁷ To elaborate on the influence of the V-V distances on the magnetic ordering, we carried out additional calculations by increasing or decreasing the inter-layered V-V distances among $(V_4)_2\text{Pen}_3$. The energy differences between FM and AFM are presented in Fig. 3(c) as a function of inter-layered V-V distance. The magnetic ordering of inter-layered V atoms in $(V_4)_2\text{Pen}_3$ switches from AFM to FM when the inter-layered V-V distances shrink, while it retains AFM as the distances are further elongated. In contrast, the two intra-layered V dimers are always AFM coupled regardless of inter-layered V-V distances. In addition, we explore the exchange integrals of the intra-layered (J_1) and inter-layered (J_2) V dimers according to the classical Heisenberg model below (Eq. (2)). As shown in Fig. 3(d), the exchange integral J_2 becomes positive when the inter-layered V-V distance decreases from the equilibrium distance. Therefore, the inter-layered V atoms switch to FM spin state. Meanwhile, the inter-layered V atoms still prefer AFM coupling even though the inter-layered V-V distances are further elongated since J_2 remains negative. But J_1 varies between -3.38 and -13.15 meV, and does not change its sign, indicating that the two intra-layered V dimers always prefer AFM coupling no matter whether the inter-layered

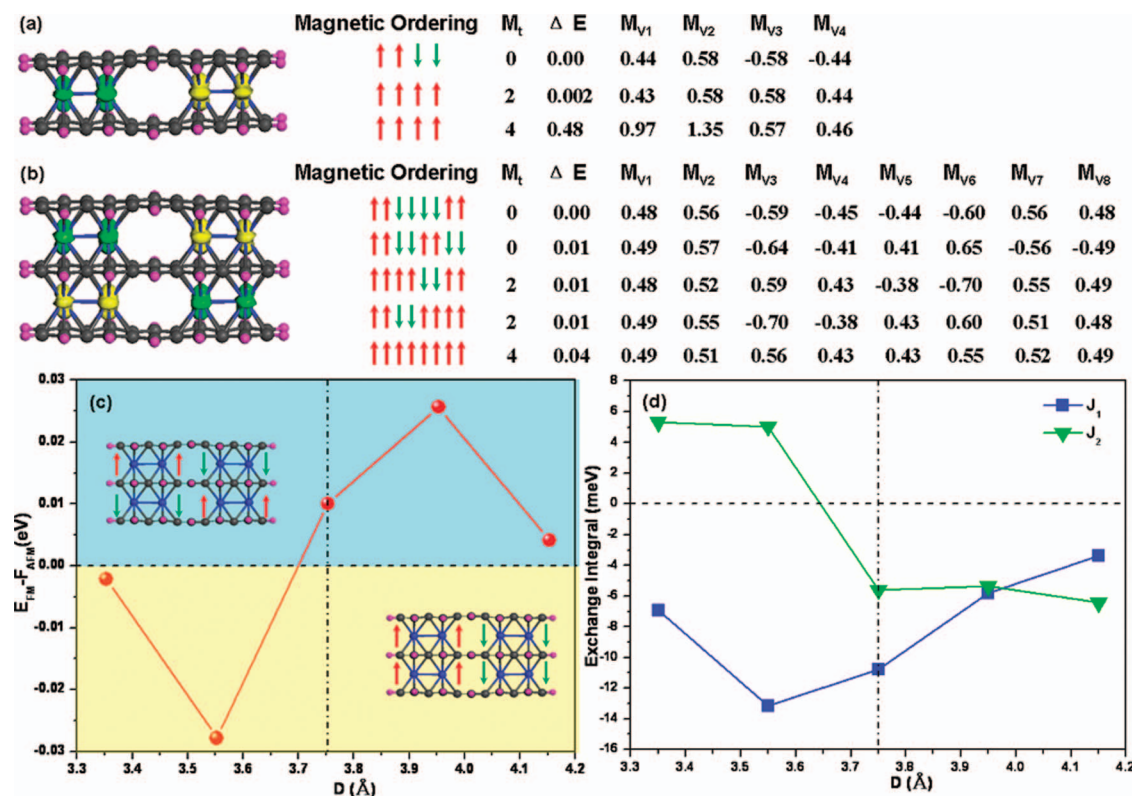


FIG. 3. Spin densities of the ground states of $V_4\text{Pen}_2$ (a) and $(V_4)_2\text{Pen}_3$ (b) sandwich clusters. The magnetic orderings, total magnetic moment M_t (μ_B), energy differences ΔE (eV), and local magnetic moment acting on each V atom (M_{V1} - M_{V8} (μ_B)) of the ground state and low-lying isomers of $V_4\text{Pen}_2$ and $(V_4)_2\text{Pen}_3$ are shown in the right column. The relative energies between FM and AFM spin states as a function of the inter-layered V-V distances of $(V_4)_2\text{Pen}_3$ are presented (c) as well as the exchange integrals J_1 and J_2 (d). The dashed-dotted line stands for equilibrium inter-layered V-V distance (3.75 \AA) of the lowest energy structure of $(V_4)_2\text{Pen}_3$. And the red and green arrows represent spin up and spin down, respectively.

V-V distances are lengthened or shortened. These phenomena are in agreement with the results shown in Fig. 3(c).

The complex magnetism of $(V_4)_n\text{Pen}_{n+1}$ clusters can also be understood from their constituent subunits. The $V_4\text{Pen}_2$ cluster can be regarded as two $V_2\text{Np}_2$ ($V_2\text{Np}_{2-1}$, $V_2\text{Np}_{2-2}$) clusters being linked side by side. Meanwhile, the middle part (V_2 , V_3 , and ligands) can be viewed as a subunit of $V_2\text{Ant}_2$. Thus, the magnetic ordering of V atoms of $(V_4)_n\text{Pen}_{n+1}$ can be inferred by the magnetic coupling in the subunits of $V_2\text{Np}_2$ and $V_2\text{Ant}_2$. For the isolated V dimer, the two V atoms favor FM coupling⁶⁸ due to direct metal-metal interactions. When the V_2 dimer is sandwiched by two naphthalene ligands, the local magnetic moments on two V atoms are still aligned in parallel.⁶⁹ Thus, the first two V atoms (V_1 and V_2) and the last two V atoms (V_3 and V_4) in the structure of $(V_4)_n\text{Pen}_{n+1}$ are FM coupled, respectively, via the direct exchange interaction. However, as the distance between two V atoms increases, the direct exchange integral decreases rapidly, and the indirect superexchange interaction becomes dominant in determining the magnetic ordering of V atoms, e.g., the two V atoms are AFM coupled in both $V_2\text{Ant}_2$,²⁴ so do the V_2 and V_3 atoms in $V_4\text{Pen}_2$. We believe that the FM coupling between the V_1 (V_3) and V_2 (V_4) is due to the direct exchange interaction while the AFM coupling between the pairs of (V_1 - V_2) and (V_3 - V_4) is a result of Pen mediated superexchange interaction for $V_4\text{Pen}_2$. As for the multidecker $(V_4)_2\text{Pen}_3$ cluster, the intra-layered V atoms behave similarly to those of $V_4\text{Pen}_2$, where V_1 (V_3) and V_2 (V_4) are FM coupled but the V_1 - V_2 pair is AFM coupled with the V_3 - V_4 pair. Meanwhile, the inter-layered V-V pairs are also AFM coupled. Compared with those of $(V_3)_2\text{Pen}_3$ (3.64 or 3.81 Å), the distances of inter-layered V atoms in $(V_4)_2\text{Pen}_3$ (3.75 or 3.84 Å) (Fig. 1) are elongated, which weakens the direct exchange interaction between them while the V-Pen distances are shortened (1.82 Å in $(V_4)_2\text{Pen}_3$ vs 1.87 Å in $(V_3)_2\text{Pen}_3$), which also enhances the interaction in V-Pen, leading to the superexchange prevailing over the direct exchange interaction and thus AFM coupling is favored between the inter-layered V atoms in $(V_4)_2\text{Pen}_3$. Therefore, we can conclude that the FM or AFM coupling of the intra-layered V atoms is ascribed to the direct exchange or superexchange interaction, whereas there is competition of direct exchange and superexchange interactions for inter-layered V atoms in both $(V_3)_n\text{Pen}_{n+1}$ and $(V_4)_n\text{Pen}_{n+1}$ clusters.

The exchange integrals are estimated through the classical Heisenberg Hamiltonian of the following form:

$$H = E_0 - J_1 \sum_{\langle i,j \rangle_1} \vec{S}_i \cdot \vec{S}_j - J_2 \sum_{\langle i,j \rangle_2} \vec{S}_i \cdot \vec{S}_j, \quad (2)$$

where $\langle i,j \rangle_1$ and $\langle i,j \rangle_2$ represent the summations over the two neighboring intra-layered (e.g., V_1 and V_2 in Fig. 1(c)) and inter-layered V atoms (e.g., V_1 and V_4 in Fig. 1(c)), respectively; S_i denotes the spin localized on atom i . It should be noted that the two nearest intra-layered V atoms are treated as one unit in $(V_4)_n\text{Pen}_{n+1}$ clusters since they always show the same spin direction. With the knowledge of J_1 and J_2 , we obtain the critical temperature of finite clusters through Monte Carlo simulations. The predicted critical temperatures for $V_3\text{Pen}_2$, $(V_3)_2\text{Pen}_3$, $V_4\text{Pen}_2$, and $(V_4)_2\text{Pen}_3$ are 288, 110, 9, and 32 K, respectively (see the supplementary material⁵¹).

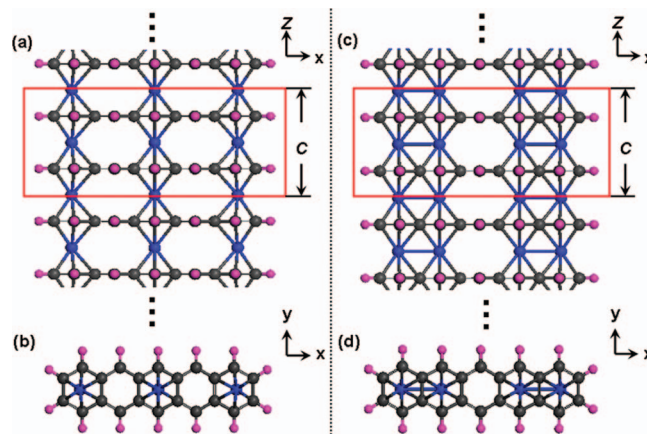


FIG. 4. Side [(a) and (c)] and top views [(b) and (d)] of 1D molecular wires $[V_3\text{Pen}]_\infty$ and $[V_4\text{Pen}]_\infty$. The red line rectangles represent the $1 \times 1 \times 2$ supercells for these two wires.

B. Molecular wire

Besides the finite V-Pen sandwich clusters, their infinite 1D molecular wires $[V_3\text{Pen}]_\infty$ and $[V_4\text{Pen}]_\infty$ are also explored. A $1 \times 1 \times 2$ supercell is used to identify both the FM and AFM magnetic ordering as shown in Fig. 4. The energetically most favored structures are the FM states with very high magnetic moments of $6.8 \mu_B$ and $4.0 \mu_B$ per unit cell for $[V_3\text{Pen}]_\infty$ and $[V_4\text{Pen}]_\infty$, respectively (see the supplementary material⁵¹). Their ferrimagnetic or AFM states are much less stable than the FM states and are about 0.57 eV and 0.12 eV higher in energy. The lattice constant c along the periodic directions for optimized $[V_3\text{Pen}]_\infty$ and $[V_4\text{Pen}]_\infty$ molecular wires are 7.11 and 7.16 Å, respectively. The BEs of $[V_3\text{Pen}]_\infty$ and $[V_4\text{Pen}]_\infty$, with respect to individual Pen and isolated metal atom, are as large as 12.0 and 16.0 eV per unit cell, respectively, indicating that these infinite 1D molecular wires are highly stable. It must be pointed out that our DFT calculations at 0 K yield ferromagnetism in 1D nanowires, but V-V may not achieve ferromagnetic ordering under finite temperature according to the Mermin-Wagner theorem,⁷⁰ because the classical Heisenberg model employed in current study is only for short range interaction. To investigate how the interaction varies with respect to distance we need to employ a much larger system, which may be one of our future works when our computational facility is available.

As discussed above, the energetically most favorable states of $[V_3\text{Pen}]_\infty$ and $[V_4\text{Pen}]_\infty$ are FM coupled, which the spins on the intra-layered and inter-layered V atoms are all aligned in a parallel order. This contrasts to the diverse magnetic orderings in the finite clusters. The FM coupling of V atoms leads to the extremely high magnetic moments of 6.8 and $4.0 \mu_B$ per unit cell for $[V_3\text{Pen}]_\infty$ and $[V_4\text{Pen}]_\infty$ wires, respectively. Similar transition of magnetic ordering from AFM coupling in finite $(V_2)_n\text{Ant}_{n+1}$ clusters to FM coupling in the infinite $[V_2\text{Ant}]_\infty$ wire was also observed, where two intra-layered V atoms prefer AFM coupling in $(V_2)_n\text{Ant}_{n+1}$ clusters when $n = 1$ and 2, but they favor FM coupling in larger clusters when $n \geq 3$ and in the infinite molecular wire $[V_2\text{Ant}]_\infty$.²⁴ The transition from AFM in the finite $(V_4)_2\text{Pen}_3$ cluster to FM in $[V_4\text{Pen}]_\infty$ is a consequence of the

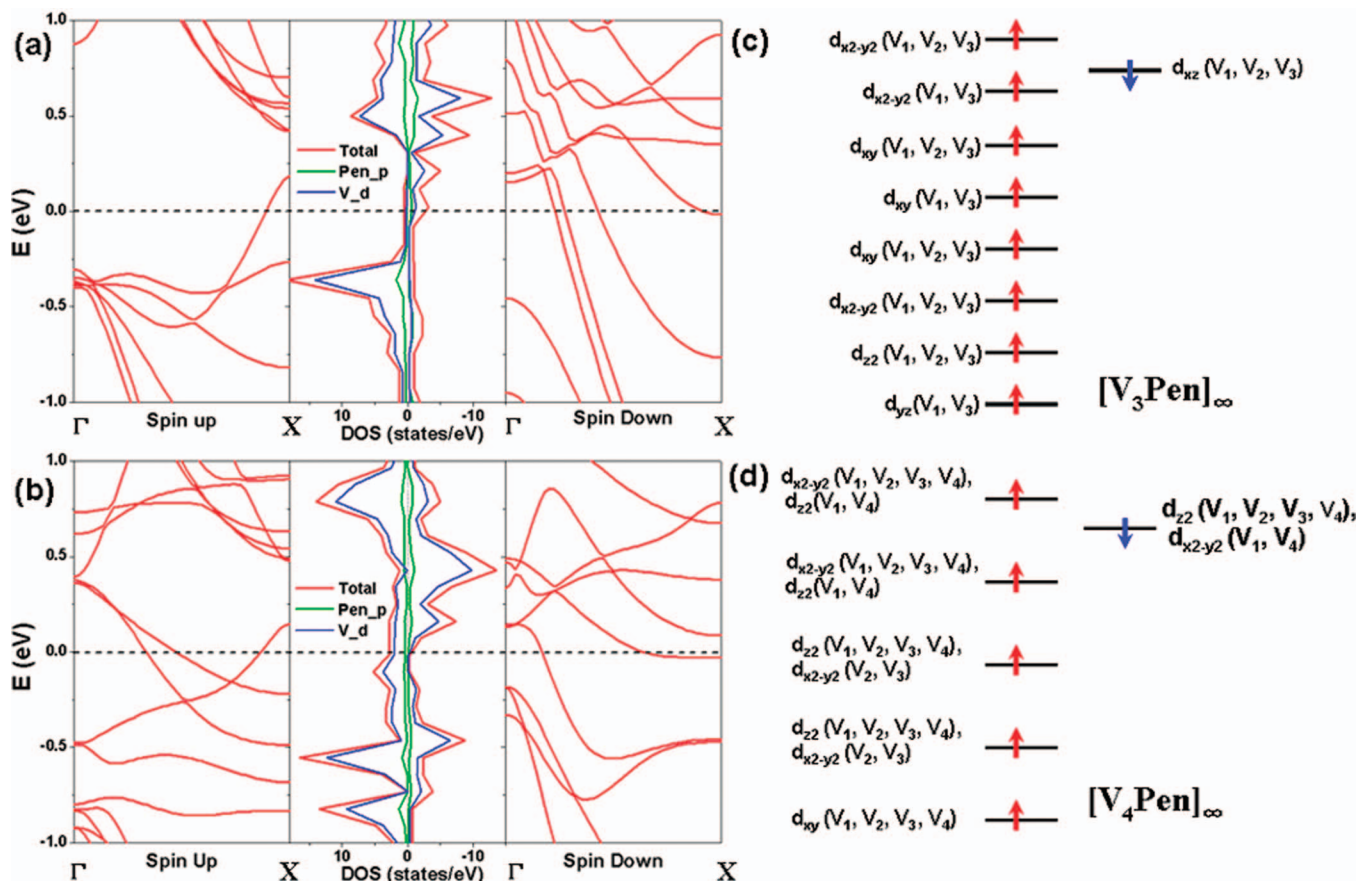


FIG. 5. The band structure and DOS of $[V_3\text{Pen}]_\infty$ (a) and $[V_4\text{Pen}]_\infty$ (b). The left and right columns present the spin up and down band structures, respectively. While the DOS is plotted in the middle column; the green and blue solid lines correspond to the p states of ligand and d states of V atom; other components, namely, the s states of ligand and V atom and the p states of V atom are not shown since their contribution in this energy range are nearly zero. Schematic diagram of net valence electron configurations at the gamma (Γ) point of the lowest energy structures of $[V_3\text{Pen}]_\infty$ (c) and $[V_4\text{Pen}]_\infty$ (d). The red and blue arrows represent the spin up and down electrons, respectively.

competition between direct exchange and superexchange interactions. In the infinite $[V_4\text{Pen}]_\infty$ wire, the inter-layered V-V distance is 3.58 Å, which is shorter than that of 3.75 or 3.84 Å in $(V_4)_2\text{Pen}_3$ by ~ 0.2 Å (Fig. 1). As we have established in the finite $(V_4)_2\text{Pen}_3$ cluster, the magnetic ordering changes from AFM to FM when the inter-layered V-V distances are decreased, which might suggest that the direct exchange in infinite wire is stronger than that in the finite cluster. This results in the direct exchange to be predominant over the superexchange, and FM eventually would be more favorable than AFM coupling. In addition, the magnetic moments of these molecular wires are much larger ($[V_3\text{Pen}]_\infty$ ($6.8 \mu_B$ per unit cell), $[V_4\text{Pen}]_\infty$ ($4.0 \mu_B$ per unit cell)) than those in the mononuclear molecular wires $[\text{VBz}]_\infty$,¹⁰ $[\text{ScCp}]_\infty$,¹⁶ $[\text{TiCp}]_\infty$,¹⁶ and $[\text{NbBz}]_\infty$.¹⁶ The high magnetism and the high stable spin states of these infinite molecular wires show that they can be good candidates for magnetic storage materials.

The band structures, density of states (DOS), and schematic diagram of the net valence electron configurations at the gamma (Γ) point of the ground states of $[V_3\text{Pen}]_\infty$ and $[V_4\text{Pen}]_\infty$ wires are displayed in Fig. 5. It can be seen that both $[V_3\text{Pen}]_\infty$ and $[V_4\text{Pen}]_\infty$ are FM metals with several bands crossing the Fermi levels. Note that only one band crosses the Fermi level in the spin-up channel while there are four bands in the spin-down channel across the Fermi

level in $[V_3\text{Pen}]_\infty$. This demonstrates that the molecular wire $[V_3\text{Pen}]_\infty$ possesses large spin polarization around the Fermi level, which can also be justified from the DOS shown in the middle column of Fig. 5(a). Besides, the p states of Pen and the d states of V atoms are strongly hybridized, which accounts for the high stability of both wires. The schematic diagram of the net valence electron configurations (Figs. 5(c) and 5(d)) can account for the ultra high magnetic moments of these two molecular wires. In the case of $[V_3\text{Pen}]_\infty$, the net eight spin-up electrons occupy the $d_{x^2-y^2}$, d_{xy} , and d_{z^2} orbitals which are contributed mainly from three V_1 , V_2 , and V_3 atoms and $d_{x^2-y^2}$, d_{xy} , and d_{yz} orbitals from V_1 and V_3 atoms; while its net one spin-down electron occupies the d_{xz} orbital mainly from V_1 , V_2 , and V_3 atoms. Consequently, the total net magnetic moment is close to $7.0 \mu_B$ per unit cell for $[V_3\text{Pen}]_\infty$, which is in good agreement with the calculated value of $6.8 \mu_B$. As for $[V_4\text{Pen}]_\infty$, the $d_{x^2-y^2}$, d_{z^2} , and d_{xy} bands from V_1 , V_2 , V_3 , and V_4 atoms, d_{z^2} band from V_1 and V_4 atoms, and $d_{x^2-y^2}$ bands from V_2 and V_3 atoms are occupied by five spin-up electrons, whereas the spin-down electron occupies the band dominated from the d_{z^2} component of V_1 , V_2 , V_3 , and V_4 atoms and $d_{x^2-y^2}$ component of V_1 and V_4 atoms. Clearly, the total net magnetic moment ($4.0 \mu_B$), which is inferred from Fig. 5(d), matches exactly with the calculated value ($4.0 \mu_B$).

IV. CONCLUSION

In summary, we have systematically studied the structural, electronic, and magnetic properties of $(V_3)_n\text{Pen}_{n+1}$ and $(V_4)_n\text{Pen}_{n+1}$ ($n = 1, 2$) sandwich clusters and their infinite 1D molecular wires $[V_3\text{Pen}]_\infty$ and $[V_4\text{Pen}]_\infty$ using spin-polarized DFT approach. Our calculations show that these clusters and infinite 1D molecular wires are stable against decomposition into small fragments and should be accessible experimentally. More importantly, we elucidate the magnetic coupling mechanisms among these structures; i.e., the neighboring intra-layered V atoms are AFM coupled for $(V_3)_n\text{Pen}_{n+1}$ through the superexchange interaction, whereas they can be either FM or AFM coupled for $(V_4)_n\text{Pen}_{n+1}$ via the direct exchange or superexchange interaction. In contrast, the inter-layered V atoms favor FM coupling in $(V_3)_2\text{Pen}_3$ and AFM coupling for $(V_4)_2\text{Pen}_3$ depending on the competition between direct exchange and superexchange interactions mediated by the Pen ligands. However, the infinite 1D $[V_3\text{Pen}]_\infty$ and $[V_4\text{Pen}]_\infty$ molecular wires are both FM metals with large magnetic moments, and $[V_3\text{Pen}]_\infty$ exhibits large spin polarization around the Fermi level. Hence, they might have a wide potential application in future spintronic devices.

It may be worthy to note that from the reflection absorption spectroscopic experiment⁷¹ VBz₂ sandwich cluster has no orientational preference when it is deposited onto a bare gold substrate due to the weak interaction between Bz and the substrate, which limits its practical application in the assembly of nanodevices. On the other hand, the Pen molecule can strongly bond to suitable substrates such as the Si(100) surface,^{45,72} we can thus expect the V-Pen sandwich clusters to be able to be effectively deposited onto the substrate with controllable orientation for practical application. Though the ferromagnetism in 1D molecular wire spontaneously breaks at finite temperature if the interaction is short ranged, the finite V-Pen clusters still could be ferromagnets at finite temperature. Such ferromagnetism has been observed in the finite sandwich cluster, $V_n\text{Bz}_{n+1}$ ($n = 1-4$), at 60–300 K by Stern-Gerlach experiments.⁴ It can be expected that the ferromagnetic spin alignment can be observed in finite V-Pen sandwich clusters. Considering the unique magnetic properties of $(V_3)_n\text{Pen}_{n+1}$ and $(V_4)_n\text{Pen}_{n+1}$ sandwich clusters, tuning the magnetic moments can be achieved by changing the sizes of these two clusters when they are absorbed on substrates, which provides a probable breakthrough in producing tunable magnetic moments nanodevices.

ACKNOWLEDGMENTS

This work is supported by the NBRP (2010CB923401, 2011CB302004, 2009CB623200), NSF (11074035, 21173040), SRDP (20090092110025), the Outstanding Yong Faculty Grant, and Peiyu Foundations of SEU in China. The authors thank the computational resource at Department of Physics, SEU.

¹C. A. Coulson, P. W. Higgs, and N. H. March, *Nature (London)* **168**, 1039 (1951).

²G. Wilkinson, M. Rosenblum, M. C. Whiting, and R. B. Woodward, *J. Am. Chem. Soc.* **74**, 2125 (1952).

- ³K. Hoshino, T. Kurikawa, H. Takeda, A. Nakajima, and K. Kaya, *J. Phys. Chem.* **99**, 3053 (1995).
- ⁴K. Miyajima, A. Nakajima, S. Yabushita, M. B. Knickelbein, and K. Kaya, *J. Am. Chem. Soc.* **126**, 13202 (2004).
- ⁵R. Takegami, N. Hosoya, J.-i. Suzumura, A. Nakajima, and S. Yabushita, *J. Phys. Chem. A* **109**, 2476 (2005).
- ⁶N. Hosoya, R. Takegami, J.-i. Suzumura, K. Yada, K. Koyasu, K. Miyajima, M. Mitsui, M. B. Knickelbein, S. Yabushita, and A. Nakajima, *J. Phys. Chem. A* **109**, 9 (2004).
- ⁷K. Miyajima, M. B. Knickelbein, and A. Nakajima, *Eur. Phys. J. D* **34**, 177 (2005).
- ⁸K. Miyajima, M. B. Knickelbein, and A. Nakajima, *J. Phys. Chem. A* **112**, 366 (2008).
- ⁹L. Y. Zhu, J. L. Wang, and M. L. Yang, *J. Mol. Struct.: THEOCHEM* **869**, 37 (2008).
- ¹⁰H. J. Xiang, J. L. Yang, J. G. Hou, and Q. S. Zhu, *J. Am. Chem. Soc.* **128**, 2310 (2006).
- ¹¹L. P. Zhou, S.-W. Yang, M.-F. Ng, M. B. Sullivan, B. C. Vincent, and L. Shen, *J. Am. Chem. Soc.* **130**, 4023 (2008).
- ¹²X. Y. Zhang and J. L. Wang, *J. Phys. Chem. A* **114**, 2319 (2010).
- ¹³J. L. Wang, P. H. Acioli, and J. Jellinek, *J. Am. Chem. Soc.* **127**, 2812 (2005).
- ¹⁴X. Y. Zhang, M.-F. Ng, Y. B. Wang, J. L. Wang, and S.-W. Yang, *ACS Nano* **3**, 2515 (2009).
- ¹⁵X. Y. Zhang, J. L. Wang, Y. Gao, and X. C. Zeng, *ACS Nano* **3**, 537 (2009).
- ¹⁶L. Shen, S.-W. Yang, M.-F. Ng, V. Ligatchev, L. P. Zhou, and Y. P. Feng, *J. Am. Chem. Soc.* **130**, 13956 (2008).
- ¹⁷A. K. Kandalam, B. K. Rao, P. Jena, and R. Pandey, *J. Chem. Phys.* **120**, 10414 (2004).
- ¹⁸L. Y. Zhu and J. L. Wang, *J. Phys. Chem. C* **113**, 8767 (2009).
- ¹⁹R. Pandey, B. K. Rao, P. Jena, and M. A. Blanco, *J. Am. Chem. Soc.* **123**, 3799 (2001).
- ²⁰L. Y. Zhu, T. T. Zhang, M. X. Yi, and J. L. Wang, *J. Phys. Chem. A* **114**, 9398 (2010).
- ²¹L. Shen, H. M. Jin, V. Ligatchev, S.-W. Yang, M. B. Sullivan, and Y. P. Feng, *Phys. Chem. Chem. Phys.* **12**, 4555 (2010).
- ²²T. T. Zhang, L. Y. Zhu, Z. Tian, and J. L. Wang, *J. Phys. Chem. C* **115**, 14542 (2011).
- ²³K. Xu, J. Huang, S. L. Lei, H. B. Su, F. Y. C. Boey, Q. X. Li, and J. L. Wang, *J. Chem. Phys.* **131**, 104704 (2009).
- ²⁴L. Wang, Z. X. Cai, J. Y. Wang, J. Lu, G. F. Luo, L. Lai, J. Zhou, R. Qin, Z. X. Gao, D. P. Yu, G. P. Li, W. N. Mei, and S. Sanvito, *Nano Lett.* **8**, 3640 (2008).
- ²⁵L. Wang, X. F. Gao, X. Yan, J. Zhou, Z. X. Gao, S. Nagase, S. Sanvito, Y. Maeda, T. Akasaka, W. N. Mei, and J. Lu, *J. Phys. Chem. C* **114**, 21893 (2010).
- ²⁶T. Murahashi, M. Fujimoto, M.-a. Oka, Y. Hashimoto, T. Uemura, Y. Tsumi, Y. Nakao, A. Ikeda, S. Sakaki, and H. Kurosawa, *Science* **313**, 1104 (2006).
- ²⁷T. Murahashi, R. Inoue, K. Usui, and S. Ogoshi, *J. Am. Chem. Soc.* **131**, 9888 (2009).
- ²⁸T. Murahashi, M. Fujimoto, Y. Kawabata, R. Inoue, S. Ogoshi, and H. Kurosawa, *Angew. Chem., Int. Ed.* **46**, 5440 (2007).
- ²⁹T. Murahashi, K. Usui, R. Inoue, S. Ogoshi, and H. Kurosawa, *Chem. Sci.* **2**, 117 (2011).
- ³⁰T. Murahashi, Y. Hashimoto, K. Chiyoda, M. Fujimoto, T. Uemura, R. Inoue, S. Ogoshi, and H. Kurosawa, *J. Am. Chem. Soc.* **130**, 8586 (2008).
- ³¹A. P. Sergeeva and A. I. Boldyrev, *Phys. Chem. Chem. Phys.* **12**, 12050 (2010).
- ³²P. Jin, F. Y. Li, and Z. F. Chen, *J. Phys. Chem. A* **115**, 2402 (2011).
- ³³A. Muñoz-Castro and R. Arratia-Pérez, *J. Phys. Chem. A* **114**, 5217 (2010).
- ³⁴A. Muñoz-Castro, D. M.-L. Carey, and R. Arratia-Pérez, *J. Chem. Phys.* **132**, 164308 (2010).
- ³⁵J. Muñoz, L. E. Sansores, A. Martínez, and R. Salcedo, *J. Mol. Model.* **14**, 417 (2008).
- ³⁶G. E. Froudakis, A. N. Andriotis, and M. Menon, *Chem. Phys. Lett.* **350**, 393 (2001).
- ³⁷A. E. Ashley, R. T. Cooper, G. G. Wildgoose, J. C. Green, and D. O'Hare, *J. Am. Chem. Soc.* **130**, 15662 (2008).
- ³⁸J. E. Ellis, D. W. Blackburn, P. Yuen, and M. Jang, *J. Am. Chem. Soc.* **115**, 11616 (1993).
- ³⁹M. R. Philpott and Y. Kawazoe, *Chem. Phys.* **337**, 55 (2007).
- ⁴⁰T. J. Katz and N. Acton, *J. Am. Chem. Soc.* **94**, 3281 (1972).

- ⁴¹T. J. Katz, N. Acton, and J. McGinnis, *J. Am. Chem. Soc.* **94**, 6205 (1972).
- ⁴²X. J. Wu and X. C. Zeng, *J. Am. Chem. Soc.* **131**, 14246 (2009).
- ⁴³Y. Mokrousov, N. Atodiresei, G. Bihlmayer, S. Heinze, and S. Blügel, *Nanotechnology* **18**, 495402 (2007).
- ⁴⁴W. H. Mills and M. Mills, *J. Chem. Soc., Trans.* **101**, 2194 (1912).
- ⁴⁵D. Choudhary, P. Clancy, and D. R. Bowler, *Surf. Sci.* **578**, 20 (2005).
- ⁴⁶A. D. Becke, *J. Chem. Phys.* **88**, 2547 (1988).
- ⁴⁷C. Lee, W. Yang, and R. G. Parr, *Phys. Rev. B* **37**, 785 (1988).
- ⁴⁸B. Delley, *J. Chem. Phys.* **92**, 508 (1990).
- ⁴⁹B. Delley, *J. Chem. Phys.* **113**, 7756 (2000).
- ⁵⁰F. L. Hirshfeld, *Theor. Chem. Acc.* **44**, 129 (1977).
- ⁵¹See supplementary material at <http://dx.doi.org/10.1063/1.4759505> for further results.
- ⁵²X. Y. Zhang, J. L. Wang, and X. C. Zeng, *J. Phys. Chem. A* **113**, 5406 (2009).
- ⁵³A. M. James, P. Kowalczyk, E. Langlois, M. D. Campbell, A. Ogawa, and B. Simard, *J. Chem. Phys.* **101**, 4485 (1994).
- ⁵⁴X. Y. Wu and A. K. Ray, *J. Chem. Phys.* **110**, 2437 (1999).
- ⁵⁵P. R. R. Langridge-Smith, M. D. Morse, G. P. Hansen, R. E. Smalley, and A. J. Merer, *J. Chem. Phys.* **80**, 593 (1984).
- ⁵⁶T. Kurikawa, H. Takeda, M. Hirano, K. Judai, T. Arita, S. Nagao, A. Nakajima, and K. Kaya, *Organometallics* **18**, 1430 (1999).
- ⁵⁷E. L. Muetterties, J. R. Bleeke, E. J. Wucherer, and T. Albright, *Chem. Rev.* **82**, 499 (1982).
- ⁵⁸G. Kresse and J. Hafner, *Phys. Rev. B* **48**, 13115 (1993).
- ⁵⁹G. Kresse and J. Furthmüller, *Comp. Mater. Sci.* **6**, 15 (1996).
- ⁶⁰J. P. Perdew, K. Burke, and M. Ernzerhof, *Phys. Rev. Lett.* **77**, 3865 (1996).
- ⁶¹P. E. Blöchl, *Phys. Rev. B* **50**, 17953 (1994).
- ⁶²G. Kresse and D. Joubert, *Phys. Rev. B* **59**, 1758 (1999).
- ⁶³H. J. Monkhorst and J. D. Pack, *Phys. Rev. B* **13**, 5188 (1976).
- ⁶⁴J. B. Goodenough, *J. Phys. Chem. Solids* **6**, 287 (1958).
- ⁶⁵J. Kanamori, *J. Phys. Chem. Solids* **10**, 87 (1959).
- ⁶⁶V. V. Maslyuk, A. Bagrets, V. Meded, A. Arnold, F. Evers, M. Brandbyge, T. Bredow, and I. Mertig, *Phys. Rev. Lett.* **97**, 097201 (2006).
- ⁶⁷Z. H. Zhang, X. J. Wu, W. L. Guo, and X. C. Zeng, *J. Am. Chem. Soc.* **132**, 10215 (2010).
- ⁶⁸E. M. Spain and M. D. Morse, *J. Phys. Chem.* **96**, 2479 (1992).
- ⁶⁹H. S. Kang, *J. Phys. Chem. A* **109**, 9292 (2005).
- ⁷⁰P. Bruno, *Phys. Rev. Lett.* **87**, 137203 (2001).
- ⁷¹M. Mitsui, S. Nagaoka, T. Matsumoto, and A. Nakajima, *J. Phys. Chem. B* **110**, 2968 (2006).
- ⁷²W. A. Hofer, A. J. Fisher, G. P. Lopinski, and R. A. Wolkow, *Phys. Rev. B* **63**, 085314 (2001).